

**GA-A27300**

**PEDESTAL MAGNETIC FIELD MEASUREMENTS  
USING A MOTIONAL STARK EFFECT POLARIMETER**

by  
M.J. LANCTOT, C.T. HOLCOMB, S.L. ALLEN, M.E. FENSTERMACHER,  
and T.C. LUCE

**MAY 2012**



## DISCLAIMER

This report was prepared as an account of work sponsored by an agency of the United States Government. Neither the United States Government nor any agency thereof, nor any of their employees, makes any warranty, express or implied, or assumes any legal liability or responsibility for the accuracy, completeness, or usefulness of any information, apparatus, product, or process disclosed, or represents that its use would not infringe privately owned rights. Reference herein to any specific commercial product, process, or service by trade name, trademark, manufacturer, or otherwise, does not necessarily constitute or imply its endorsement, recommendation, or favoring by the United States Government or any agency thereof. The views and opinions of authors expressed herein do not necessarily state or reflect those of the United States Government or any agency thereof.

GA-A27300

# PEDESTAL MAGNETIC FIELD MEASUREMENTS USING A MOTIONAL STARK EFFECT POLARIMETER

by  
M.J. LANCTOT,\* C.T. HOLCOMB,\* S.L. ALLEN,\* M.E. FENSTERMACHER,\*  
and T.C. LUCE

This is a preprint of a paper to be presented at the Nineteenth High Temperature Plasma Diagnostics Conference, May 6-10, 2012 in Monterey, California and to be submitted for publication in *Rev. Sci. Instrum.*

\*Lawrence Livermore National Laboratory, Livermore, California.

Work supported by  
the U.S. Department of Energy  
under DE-AC52-07NA27344 and DE-FC02-04ER54698

GENERAL ATOMICS PROJECT 30200  
MAY 2012





# Pedestal Magnetic Field Measurements Using a Motional Stark Effect Polarimeter<sup>a)</sup>

M.J. Lanctot,<sup>1,b</sup> C.T. Holcomb,<sup>1</sup> S.L. Allen,<sup>1</sup> M.E. Fenstermacher,<sup>1</sup> and T.C. Luce<sup>2</sup>

<sup>1</sup>Lawrence Livermore National Laboratory, Livermore, California, USA

<sup>2</sup>General Atomics, San Diego, California, USA

(Presented XXXXX; received XXXXX; accepted XXXXX; published online XXXXX)

(Dates appearing here are provided by the Editorial Office)

Temperature-controlled, 0.15 nm interference filters were installed on an edge-viewing system of the motional Stark effect polarimeter on the DIII-D tokamak. The upgraded system provides linear control of the filter wavelength, which is important for operation in discharges where the populations of the excited states are not expected to be in statistical equilibrium. In this case, the inferred polarization angle displays a dependence on the mix of detected polarization states. Recent measurements from the calibrated edge-viewing system show increased agreement with other MSE arrays.

## I. INTRODUCTION

In the DIII-D tokamak, accurate reconstructions of the internal magnetic field rely on measurements from a motional Stark effect (MSE) polarimeter.<sup>1-4</sup> The system views the Balmer  $\alpha$  emission from a deuterium neutral beam injected at 81 kV into the midplane region of a magnetized plasma of strength 2 tesla. The beam consists of mono-, di-, and tri-molecular deuterium atoms so that three different energy components contribute to the active beam emission. Due to the motional Stark effect, the Balmer  $\alpha$  line ( $n=3$  to 2 transition for principle quantum number  $n$ ) for each energy component is split into six  $\pi$  components polarized along the electric field direction, and three  $\sigma$  components polarized perpendicular to the electric field. Six other transitions are possible, but due to their weaker intensities are not usually observed. In DIII-D, the internal magnetic field is inferred from measurements of the polarization angle of the full-energy  $\sigma$  components. The measured profile extends from the high field side of the magnetic axis out toward the plasma edge on the low field side. There is a high level of confidence in core MSE measurements owing to previous validations of the measurements.<sup>5,6</sup> Compared to the core, MSE measurements in the pedestal must be considerably more precise and accurate due to the subtle variation in the edge magnetic field, the presence of a strong edge electric field in discharges where pedestal measurements are relevant, and to the complex Stark-split deuterium alpha spectrum there. The initial edge MSE system design was guided by these considerations.<sup>4</sup> However, due to unexplained inconsistencies between edge MSE data and other measurements, edge MSE data have not been used routinely in plasma equilibrium reconstructions where the edge plasma current is of prime importance.

Recent hardware modifications to the edge MSE system have been made to address various issues including the dependence of the inferred MSE pitch angle on the mix of detected Stark states under conditions where the populations of the excited states are not expected to be in statistical equilibrium.

(Lack of statistical equilibrium means the sublevels within the manifold of a principle quantum number are not equally populated.) This was done in two ways: by increasing both the precision of the wavelength calibration and the polarization fraction of the detected emission using temperature-controlled, narrow (~0.15 nm) bandpass filters. This initial scoping study was done on only nine edge MSE channels. Analysis of recent data shows a reduction in the dependence of the inferred polarization angle on the mix of detected Stark states, and increased agreement in the measured vertical field between the edge system and other MSE arrays.

## II. WAVELENGTH CALIBRATION

The measurement of the Balmer  $\alpha$  spectrum is spatially localized to the intersection of the sightline and the neutral beam. The observation geometry, beam voltage, and magnetic field strength determine the central wavelength of the Doppler-shifted Stark-split emission. In the original polarimeter design for the edge array (Fig. 5 in Ref. 4), the interference filter was tuned to the desired  $\sigma$  wavelength by varying the angle of incidence of the light passing through the filter. This method exploits the nonlinear dependence of the filter bandpass on the angle of incidence where a non-zero angle results only in a blue shift. By tilting the filter, the filter bandpass is scanned across the  $\sigma$  and  $\pi$  components resulting in a polarization spectrum.<sup>7</sup> The optimal alignment occurs when the bandpass is aligned with the  $\sigma$  component and the signal intensity is maximized.

Under conditions where the upper state populations achieve statistical equilibrium, the  $\sigma$  components are polarized perpendicular to the  $\pi$  components.<sup>7</sup> In this case, the total polarization angle measured by the MSE system is not sensitive to the polarization fraction, or mix of detected  $\sigma$  and  $\pi$  components so that detection of some  $\pi$  light would reduce the signal-to-noise ratio but not change the polarization angle. This is ideal for MSE diagnostics since detection of some  $\pi$  light is unavoidable due to the level of Stark splitting under typical plasma conditions.

Previous analysis of polarization spectra from DIII-D has shown that the upper state populations are likely not in statistical equilibrium for densities below  $5 \times 10^{19} \text{ m}^{-3}$ .<sup>7</sup> This is supported

<sup>a)</sup>Contributed paper published as part of the Proceedings of the 19th Topical Conference on High-Temperature Plasma Diagnostics, Monterey, California, May, 2012.

<sup>b)</sup>Email address: lanctot1@llnl.gov

by recent measurements showing that the MSE polarization angle is sensitive to the filter wavelength calibration in this density range. Figure 1 shows the inferred pitch angle ( $\gamma$ ) as a function of the filter tilt angle ( $\theta$ ). The data was taken from similar plasmas where the magnetic field pitch angle was constant and the filter angle was varied in between discharges. The measured  $\gamma(\theta)$  has a dependence on  $\theta$  similar to the filter bandpass, plotted as a solid line. The horizontal dotted line marks the calculated Doppler shifted wavelength of the Balmer  $\alpha$  line based on an in-vessel spatial calibration. The vertical dashed line shows the calibrated filter tilt angle. The alignment of the two shows consistency between the spatial and wavelength calibrations. The density dependence of this effect has not yet been measured.

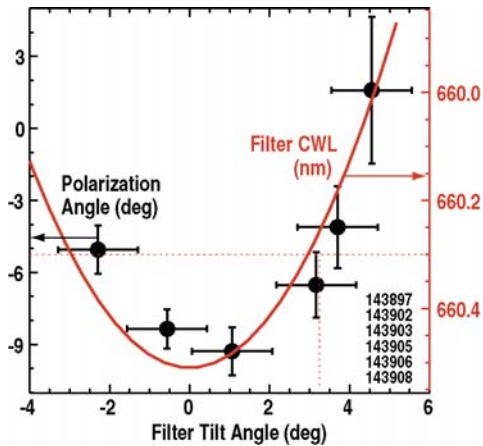


FIG. 1. Dependence of the MSE polarization angle (circles, left ordinate), and the central wavelength of the filter bandpass (line, right ordinate) on the tilt angle of a 0.3 nm bandpass interference filter. Horizontal line marks the predicted wavelength of the  $\sigma_0$  component. Vertical dotted line marks the calibrated tilt angle.

## II. SPECTRAL BROADENING

Like the core MSE system, the first generation edge MSE system used interference filters with a 0.3 nm bandwidth, which was chosen to maximize the signal-to-noise ratio (SNR) in discharges with a 2 tesla toroidal field. (The SNR was defined as the difference in the intensities of the  $\sigma$  and  $\pi$  manifolds.<sup>4</sup>) This bandwidth maximizes the SNR at the cost of the polarization fraction, which is decreased to 87% due to the proximity of the  $\sigma$  and  $\pi$  lines, and broadening effects from the MSE optics. This is illustrated in Fig. 2, which shows the predicted Stark spectrum as viewed by an edge MSE chord along with the transmission curve of the 0.3 nm filter. The spectrum was calculated for a 2 tesla discharge using measured kinetic profiles, reconstructed poloidal magnetic flux, the neutral beam geometry, MSE optic specifications, and analytic approximations of the charge-exchange cross-section effects,<sup>8</sup> and Stark line shapes.<sup>9</sup> The spectrum from a system with finite optics is broadened compared to the ideal case of a single pencil beam view because the sightlines intersect the neutral beam over a range of angles resulting in a range of observed Doppler shifts.

A low polarization fraction can explain the dependence of the polarization on the wavelength calibration as discussed in Sec. I. Installing a tall but narrow aperture in the optical train could limit the field of view in the radial direction and minimize the broadening effect. However, the existing aperture could not be easily modified. Instead, it was decided to install interference filters with a reduced bandwidth of 0.15 nm. Calculations

predicted an increase in the degree of polarization to 95% at the cost of reducing the photon flux by 50%. Calculations also showed that a filter with a sharper cutoff/on would help to discriminate the manifolds, but the resulting filter cost was prohibitive. The final design was based on a single-cavity filter in order to retain a high transmission of 60%–70%.

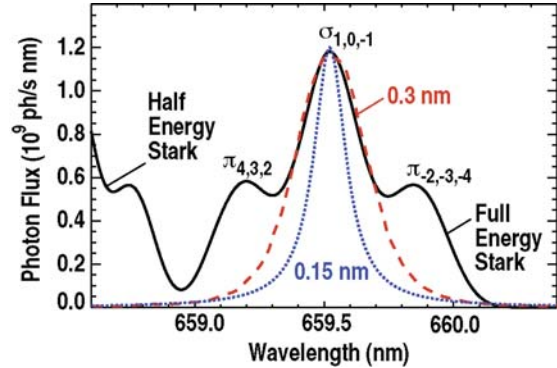


FIG. 2. Calculated Stark spectrum for a chord viewing the plasma edge (black, solid), transmission curve for a 0.3 nm bandpass filter (red, dashed) and 0.15 nm bandpass filter (blue dotted).

## III. HARDWARE SPECIFICATIONS AND CALIBRATION

When calibrating the wavelength of these narrowband filters, it is impractical to use a non-normal angle of incidence since this can increase the bandwidth and reduce the transmission. Fortunately, the filter bandpass can be tuned by controlling the filter temperature using filter ovens from Andover Corporation. In 2011, the scanning interference filter configuration was replaced by filter ovens for nine chords viewing the plasma edge. The ovens control the temperature to within 1°C from 5° above ambient ( $\sim 25^\circ\text{C}$ ) up to 60°C. The filter temperature coefficient for wavelengths near 656 nm is  $\sim 0.02$  nm/°C, which allows the bandpass to be varied by  $\pm 0.3$  nm around the design temperature. The system was calibrated to the wavelength of interest by measuring the deuterium alpha ( $D_\alpha$ ) intensity as a function of the filter wavelength, Fig. 3, in controlled discharges where quantities that affect the signal intensity such as plasma position and density were held fixed. Although the procedure requires a dozen discharges to complete,

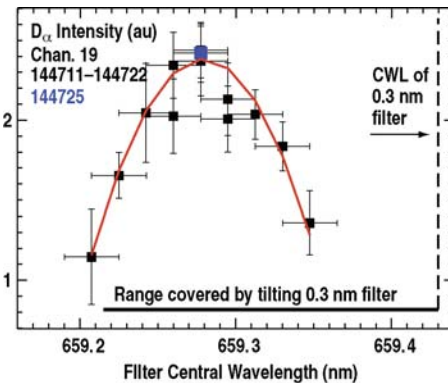


FIG. 3. Dependence of the measured  $D_\alpha$  intensity on the central filter wavelength of a temperature-controlled filter with a 0.15 nm bandpass for a chord viewing the plasma edge. Dashed vertical line marks the central wavelength of a 0.3 nm filter used

in the scanning filter configuration. The horizontal line marks the wavelength range covered by tilting the filter  $\pm 5^\circ$ .

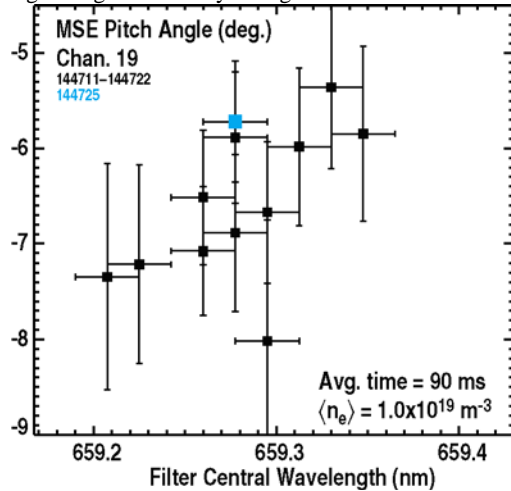


FIG. 4. Dependence of the MSE pitch angle on the central wavelength of a temperature controlled 0.15 nm filter.

all the channels can be calibrated simultaneously. The resulting calibration wavelengths are in good agreement with previous calibration results using the scanning interference filters.

The new system shows a reduced variation in the pitch angle with the filter bandpass, Fig. 4. The measurements were averaged over 90 ms in low-density ( $\sim 1.0 \times 10^{19} \text{ m}^{-3}$ ) neutral beam heated discharges. The linear trend in the pitch angle is consistent with the linear dependence of the wavelength on the filter temperature. The density dependence of the observed trend is the subject of ongoing investigation.

#### IV. INITIAL MAGNETIC FIELD MEASUREMENTS

The upgraded edge system was commissioned and calibrated during 2011. Initial magnetic field measurements from the edge system show good agreement with the tangential MSE system, which has a single view of the plasma pedestal region. Data from the two systems are compared in Fig. 5(a), which shows the time evolution of the effective vertical magnetic field ( $B_{Z0}$ ), which is the vertical field measured by the MSE system including the contribution from the plasma generated radial electric field ( $E_r$ ).<sup>10</sup> The two edge views are localized in the plasma at major radii 2.250 m and 2.254 m, and the tangential chord view is at 2.252 m as measured during an in-vessel calibration. These locations mark the centers in major radius of the sampling volumes, which are 10 cm wide for the tangential viewing system, and 3.5 mm wide for the edge-viewing system. During the low confinement mode (L-mode) phase of the discharge when the plasma generated radial electric field is small, the two systems are in good agreement. However, following the transition to the high confinement mode (H-mode), the contribution of  $E_r$  increases with the plasma rotation leading to a significant difference in  $B_{Z0}$  as measured by the two arrays. The difference is a result of the viewing geometry alone, and allows the system to simultaneously measure the  $B_Z$  and  $E_r$ . Results from equilibrium reconstructions using the upgraded system will be reported in a future publication.

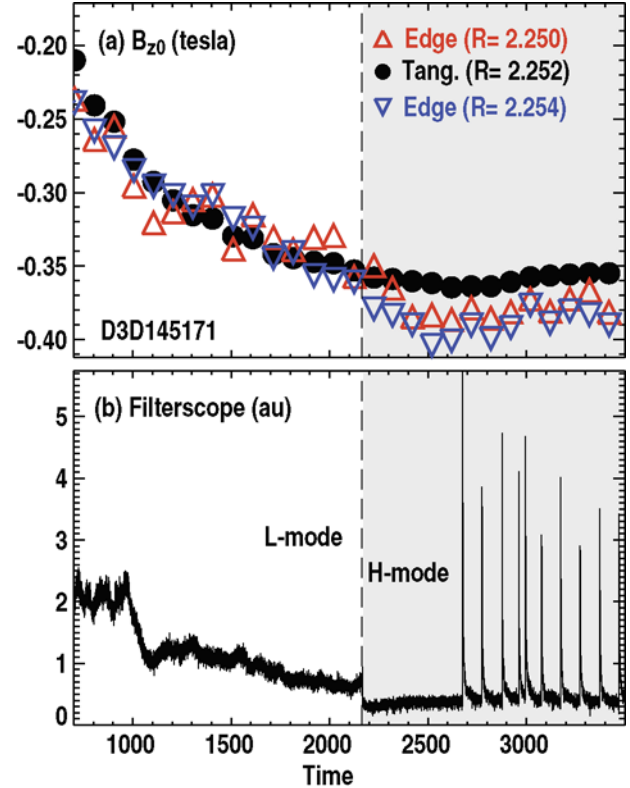


FIG. 5. Time evolution of (a)  $B_{Z0}$  as measured by the upgraded edge system (triangles), and the main tangential MSE array (circles), and (b) the  $D_\alpha$  emission in the lower divertor as measured by a filterscope system.

#### ACKNOWLEDGMENTS

This work was supported by the US Department of Energy under DE-AC52-07NA27344 and DE-FC02-04ER54698.

#### REFERENCES

- <sup>1</sup>C. T. Holcomb, M. A. Makowski, S. L. Allen, W. H. Meyer, and M. A. Van Zeeland, *Rev. Sci. Instrum.* **79**, 10F518 (2008) and references therein.
- <sup>2</sup>F. M. Levinton, R. J. Fonck, G. M., Gammel, R. Kaita, H. W. Kugel, E. T. Powell, and D. W. Roberts, *Phys. Rev. Lett.* **63**, 2060 (1989).
- <sup>3</sup>D. Wroblewski, K. H. Burrell, L. L. Lao, P. A. Politzer, and W. P. West, *Rev. Sci. Instrum.* **61**, 3552 (1990).
- <sup>4</sup>B. W. Rice, D. G. Nilson, and D. Wroblewski, *Rev. Sci. Instrum.* **66**, 373 (1995).
- <sup>5</sup>B. W. Rice, D. G. Nilson, K. H. Burrell and L. L. Lao, *Rev. Sci. Instrum.* **70**, 815 (1999).
- <sup>6</sup>M. A. Van Zeeland, M. E. Austin, T. N. Carlstrom, T. Deterly, D. K. Finkenthal, C. T. Holcomb, R. J. Jayakumar, G. J. Kramer, M. A. Makowski, G. R. McKee, R. Nazikian, W. A. Peebles, T. L. Rhodes, W.M. Solomon, and E. J. Strait, *Nucl. Fusion* **46**, S880 (2006).
- <sup>7</sup>M. F. Gu, C. T. Holcomb, R. J. Jayakuma, and S. L. Allen, *J. Phys. B: At. Mol. Opt. Phys.* **41**, 095701 (2008).
- <sup>8</sup>M. von Hellermann, P. Breger, J. Frieling, R. Konig, W. Mandl, A. Maas, and H. P. Summers, *Plasma Phys. Controlled Fusion* **37**, 71 (1995).
- <sup>9</sup>M. G. von Hellermann, E. Delabie, R. Jaspers, P. Lotte, and H. P. Summers, Proceedings of the 19th International Conference on Spectral Line Shapes, Valladolid, Spain, 2008, and American Institute of Physics AIP Conf. Proc. **15**, 187 (2008).
- <sup>10</sup>B. W. Rice, K. H. Burrell, and L. L. Lao, *Nucl. Fusion* **37**, 517 (1997).